Journal of Sound and Vibration (1998) **217**(4), 767–779
Article No. sv981800

BOUNDARY ELEMENT ANALYSIS OF MUFFLERS WITH AN IMPROVED METHOD FOR DERIVING THE FOUR-POLE PARAMETERS

T. W. Wu and P. Zhang

Department of Mechanical Engineering, University of Kentucky, Lexington, KY 40506, *U.S.A.*

AND

C. Y. R. Cheng

Nelson Industries, Inc., Stoughton, WI 53589, *U.S.A.*

(*Received* 12 *May* 1997, *and in final form* 12 *June* 1998)

When a muffler is modelled by the boundary element method (BEM), the transmission loss (TL) can be evaluated by either the conventional four-pole method or the recently developed three-point method. The three-point method produces only the transmission loss (TL), and nothing else. On the other hand, the four-pole method has the advantage of retaining the transfer matrix of the muffler, which contains important parameters when the muffler is connected to another muffler or other components in the exhaust system. However, the major drawback of the conventional four-pole method is that it requires two separate boundary element runs due to the two different boundary conditions imposed on the outlet boundary. Therefore, it can take twice as long to get the TL when compared to the more efficient three-point method. In this paper, an improved method to derive the four-pole parameters for use in the BEM is introduced. Although two boundary element runs are still needed at each frequency, the improved method only solves the boundary element matrix once at each frequency. Therefore, it is as efficient as the three-point method. More importantly, the improved method also produces the four-pole parameters. The boundary element analysis is done by the direct mixed-body BEM. Numerical predictions are compared to experimental results for all test cases, including one with a mean flow effect.

1. INTRODUCTION

Muffler performance prediction is a good example of using the boundary element method (BEM) in industrial applications. Although the interior acoustic domain of a muffler is finite, the geometry inside the muffler can be quite complicated. Internal components inside a typical muffler may include perforated tubes, thin bafflers, branched cavities, and extended inlet/outlet tubes. Modelling the complex interior acoustic domain using the three-dimensional finite elements can be a very demanding job for engineers. On the other hand, the BEM provides an easier design tool because only the surfaces need to be modelled. In a recent paper, Wu

0022–460X/98/440767 + 13 $30.00/0

and Wan [1] proposed a direct mixed-body BEM to model mufflers with complex internal geometry. In the direct mixed-body BEM, the surface of each component is classified as either a regular, or a thin, or a perforated surface. The regular surfaces include the exterior muffler chamber, the inlet/outlet tubes, and the inlet/outlet ends. The thin surfaces are the thin-wall components inside the muffler, such as the extended inlet/outlet tubes, thin baffles, flow plugs (disks), and internal connecting tubes. The perforated surfaces are designated for perforated tubes or any internal surfaces with perforation. Unlike the multi-domain BEM [2–5], the direct mixed-body BEM is a single-domain BEM and requires no tedious sub-domain definition and interface matching.

Another important feature of the direct mixed-body BEM is that it allows the use of discontinuous elements. Nodal variables can be defined inside each element, instead of on the edges of each element. Therefore, continuity at the junction of any two connecting components is not required. This means each component can be meshed independently and assembled into a model without worrying about the continuity of nodal variables at junctions. In addition, the mesh of each component may also be automatically refined as the frequency goes up. A virtual component library can then be formed, and muffler models can be assembled by using the components in the library.

Traditionally, the transmission loss (TL) of a muffler has been evaluated by the four-pole method [6, 7]. The four-pole method requires two separate boundary element runs at each frequency due to the two different boundary conditions imposed on the outlet boundary [2–5]. The first BEM run uses a zero-velocity boundary condition at the outlet, and the second BEM run switches to the zero-pressure outlet condition. Because of the two different types of boundary conditions, the boundary element matrix for each run is different and needs to be solved separately. This approach is apparently too time consuming. To speed up the TL calculation process, Wan [8] proposed a so-called ''three-point method'' (also in reference [1]) to evaluate directly the TL from sound pressures in the inlet and outlet tubes. The three-point method requires only one BEM run at each frequency, and hence is much faster than the four-pole method. However, unlike the four-pole method, the three-point method does not produce the four-pole transfer matrix. The four-pole transfer matrix contains important parameters when the muffler is connected to another muffler or other components in the exhaust system. Under some circumstances, the four-pole method may also be used to reduce the size of the problem as well as the total CPU time when a large complex muffler is divided into two or more sub-mufflers.

To overcome the shortcomings of both the four-pole method and the three-point method, an improved method for deriving the four-pole parameters is proposed. This improved method simply permutes the variables used in the conventional four-pole method in such a way that only one single BEM matrix needs to be solved at each frequency. As a consequence, the improved method is as fast as the three-point method in evaluating the TL. More importantly, it also produces the four-pole transfer matrix. In fact, this improved four-pole formulation was first proposed and used by Kim and Soedel [9–11] in a model expansion method for

three-dimensional cavity problems, although the numerical benefit of this method in the BEM was not recognized then.

For perforated tubes, a simple empirical formula for the transfer impedance proposed by Sullivan and Crocker [12] has been used in many recent BEM calculations [1, 3, 4]. This simple formula uses only frequency and porosity as the variables. In this paper, a few other empirical formulas that include the effects of wall thickness, orifice diameter, and the mean-flow Mach number [7, 13] are also tested. All the BEM predictions are compared to experimental results, including one with a mean flow effect.

2. DIRECT MIXED-BODY BEM

In this section, the direct mixed-body boundary integral formulation by Wu and Wan [1] is briefly reviewed. Let S_r, S_t, and S_p denote the regular, thin and perforated surfaces, respectively. The interior acoustic domain is denoted by Ω. Let $\mathbf{n}$ be the unit normal vector. The unit normal vector on S_r is directed into the interior acoustic domain. The unit normal vector on S_p and S_t can be directed into either side of the thin/perforated surface. The side into which $\mathbf{n}$ is directed is called the positive side.

Let p denote the sound pressure, and v_n denote the normal velocity of the surface. The $e^{+i\omega t}$ convention in steady-state linear acoustics is adopted, where $i = \sqrt{-1}$ and ω is the angular frequency. The direct mixed-body boundary integral equations are

$$\int_{S_t+S_p} \frac{\partial \psi}{\partial n}(p^+ - p^-)\,dS + \int_{S_r}\left(p\frac{\partial \omega}{\partial n} + i\rho\omega v_n \psi\right)dS = \begin{Bmatrix} 4\pi p(P), & P\in\Omega, \\ 2\pi p(P), & P\in S_r, \\ 2\pi[p^+(P)+p^-(P)], & P\in S_t+S_p, \end{Bmatrix} \tag{1a–c}$$

$$\int_{S_t+S_p} \frac{\partial^2 \psi}{\partial n\,\partial n^P}(p^+ - p^-)\,dS + \int_{S_r}\left(p\frac{\partial^2 \omega}{\partial n\,\partial n^P} + i\rho\omega v_n \frac{\partial \psi}{\partial n^P}\right)dS = \begin{Bmatrix} -4\pi i\rho\omega v_n(P), & P\in S_t, \\ 4\pi(ik/\xi)[p^+(P)-p^-(P), & P\in S_p, \end{Bmatrix} \tag{2a–b}$$

where P is the collocation point, ψ is the free-space Green's function, ρ is the mean density of the fluid, k is the wavenumber, and ξ is the non-dimensional transfer impedance for the perforated surface S_p. In the above equations, p^+ is the sound pressure on the positive side of S_t or S_p, and p^- is the sound pressure on the opposite side. The explicit expression for ψ is

$$\psi = e^{-ikr}/r, \tag{3}$$

where $r = |P - Q|$, and Q is any integration point on the boundary. In equation (2), $\partial/\partial n^P$ means partial differentiation with respect to the co-ordinates of P in the normal direction of P. It should be noted that the first integral of equation (2) is hypersingular and converges only in the Hadamard finite-part sense [14]. The hypersingular integral can be regularized by using Stokes' theorem [15]. Equations (1b), (2a) and (2b) are solved simultaneously for pressure on S_r, and pressure jump on S_t and S_p.

In equation (2b), the perforated surface is modelled by the equivalent transfer impedance approach [12]. In other words, the normal velocity on S_p is related to the pressure jump by

$$p^- - p^+ = \rho c \xi v_n. \tag{4}$$

At room temperature and under the no-flow condition, a simple empirical formula given by Sullivan and Crocker [12] for ξ in the linear regime is

$$\xi = (1/\rho c\sigma)(2{\cdot}4 + \mathrm{i}0{\cdot}02f), \tag{5}$$

where f is frequency in Hz, and σ is the porosity (the open to the total area ratio).

Equation (5) is easy to use because it contains only f and σ as the variables. Sullivan has also developed a more detailed formula that includes the effects of hole diameter and wall thickness. The formula can be found in the book by Munjal [7]:

$$\xi = (1/\sigma)[6 \times 10^{-3} + \mathrm{i}k(t + 0{\cdot}75d_h)], \tag{6}$$

where k is the wavenumber, t is the wall thickness of the perforated surface, and d_h is the hole diameter.

Another alternative formula that also includes the effects of hole diameter and wall thickness was reported by Bento Coelho [13]. The formula is

$$\xi = (1/\rho c)(R_0 + \mathrm{i}X_0), \qquad R_0 = (1/\sigma)[\rho(d'/d_h)\sqrt{8\nu\omega} + (\rho/8c)(\omega d_h)^2], \tag{7a, b}$$

$$X_0 = (\omega\rho/\sigma)(d'' + (d'/d_h)\sqrt{8\nu/\omega}), \tag{7c}$$

with

$$d' = t + d_h, \qquad d'' = t + (8/3\pi)d_h(1 - 0{\cdot}7\sqrt{\sigma}), \tag{7d, e}$$

where ν is the gas kinematic viscosity, and $\omega = 2\pi f$.

Equations (5–7) are for stationary acoustic media only. For perforates with a cross flow (or through flow), Sullivan developed a formula which can also be found in the book by Munjal [7]:

$$\xi = (1/\sigma)[0{\cdot}514d_1 M/l\sigma + \mathrm{i}0{\cdot}95k(t + 0{\cdot}75d_h)], \tag{8}$$

where d_1 is the diameter of the perforated tube, l is the length of the perforate tube, and M is the mean-flow Mach number in the tube.

For perforates with a grazing flow, Rao and Munjal [16] gave the following empirical formula:

$$\xi = (1/\sigma)[7{\cdot}337 \times 10^{-3}(1 + 72{\cdot}23M) + \mathrm{i}2{\cdot}2245 \times 10^{-5}f(1 + 51t)(1 + 204d_h)]. \tag{9}$$

Bento Coelho also developed an alternative formula for perforates with a grazing flow. That formula can be found in reference [13].

3. CONVENTIONAL FOUR-POLE METHOD

The TL of a muffler element can be computed by using the transfer matrix approach [6, 7]. With reference to Figure 1, a muffler with an inlet and an outlet can be represented by a linear acoustic four-pole network:

$$\begin{bmatrix} p_1 \\ v_1 \end{bmatrix} = \begin{bmatrix} A & B \\ C & D \end{bmatrix} \begin{bmatrix} p_2 \\ -v_2 \end{bmatrix}, \tag{10}$$

where the p_1 and v_1 are the sound pressure and normal particle velocity, respectively, at the inlet, and p_2 and v_2 are the corresponding quantities at the outlet. A negative sign on v_2 is added because the normal vector at the outlet on the BEM model is opposite to the normal at the inlet. The four-pole parameters, A, B, C, and D, can be obtained from

$$A = p_1/p_2|_{v_2=0,\, v_1=1}, \qquad B = p_1/-v_2|_{p_2=0,\, v_1=1}, \tag{11a, b}$$

$$C = v_1/p_2|_{v_2=0,\, v_1=1}, \qquad D = v_1/-v_2|_{p_2=0,\, v_1=1}. \tag{11c, d}$$

Note that the velocity boundary condition at the inlet ($v_1 = 1$) in equations (11a–d) may also be replaced by a pressure boundary condition ($p_1 = 1$). Two separate BEM runs are required to obtain the four-pole parameters at each frequency. In the first BEM run, a zero-velocity boundary condition is applied to the outlet end (i.e., $v_2 = 0$). This will produce parameters A and C. In the second BEM run, the sound pressure at the outlet end is set to zero (i.e., $p_2 = 0$). This will produce the remaining two parameters, B and D. With the four-pole parameters, A, B, C, and D, available, the TL of the muffler can then be evaluated by

$$TL = 20 \log_{10} \{\tfrac{1}{2}|A + B(1/\rho c) + C\rho c + D|\} + 10 \log_{10} S_i/S_o, \tag{12}$$

where S_i and S_o are the cross-sectional areas of the inlet and oulet tubes, respectively.

Because of the two different types of boundary conditions applied at the outlet, the two BEM runs do not share the same cofficient matrix. That means the matrix solver needs to be called twice at each frequency. This simply makes the conventional four-pole method an impractical choice for computing the TL.

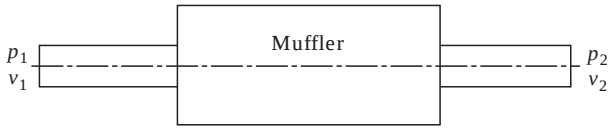

Figure 1. The four-pole method.

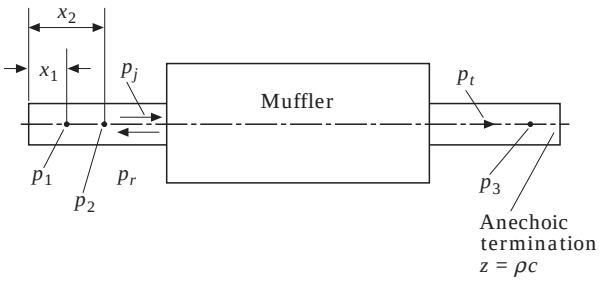

Figure 2. The three-point method.

4. THREE-POINT METHOD

Unlike the four-pole method, the three-point method [1, 8] uses only one single BEM run to compute the TL at each frequency. In this single BEM run, the inlet is still excited by a uniform velocity or pressure, while an anechoic termination (impedance equal to ρc) is used at the outlet end, as shown in Figure 2. The acoustic wave in the outlet tube contains only an outgoing wave due to the anechoic termination. The acoustic wave in the inlet tube contains an incoming wave as well as a reflected wave. Two points in the inlet tube are selected to extract the incoming wave. Let x_1 and x_2 be the longitudinal co-ordinates of the two selected points along the muffler axis, respectively. The corresponding sound pressures p_1 and p_2 at these two points can be written as

$$p_1 = p_i\, e^{-ikx_1} + p_r\, e^{ikx_1}, \qquad p_2 = p_i\, e^{-ikx_2} + p_r\, e^{ikx_2}, \tag{13a, b}$$

where p_i represents the incoming wave, and p_r represents the reflected wave. Solving equations (13a) and (13b) for p_i gives

$$p_i = (1/2i \sin [k(x_2 - x_1)])(p_1\, e^{ikx_2} - p_2\, e^{ikx_1}), \tag{14}$$

provided that $\sin [k(x_2 - x_1)] \neq 0$. As shown in Figure 2, the third point can be placed anywhere in the outlet tube. The pressure at that point is p_3. Then, the TL of the muffler can be evaluated by

$$TL = 20 \log_{10} (|p_i|/|p_3|) + 10 \log_{10} (S_i/S_o). \tag{15}$$

Compared to the four-pole method, the three-point method is indeed a much faster method for computing the TL, due to its single BEM run nature. However, the three-point method does not produce the four-pole transfer matrix. The four-pole matrix represents important characteristics of the muffler, and can be combined with other four-pole matrices when the muffler is connected to other components in the exhaust system.

5. IMPROVED METHOD TO DERIVE THE FOUR POLE PARAMETERS

From the system point of view, the four-pole method is still a desirable method. To speed up the conventional four-pole method, one can simply permute the

variables used in the four-pole network in such a way that only the velocity boundary condition is used in the BEM. Rearrange equation (10) to get

$$\begin{bmatrix} p_1 \\ p_2 \end{bmatrix} = \begin{bmatrix} A^* & B^* \\ C^* & D^* \end{bmatrix} \begin{bmatrix} v_1 \\ -v_2 \end{bmatrix}, \tag{16}$$

where

$$A^* = p_1|_{v_1=1,\, v_2=0}, \qquad B^* = p_1|_{v_1=0,\, v_2=-1}, \tag{17a, b}$$

$$C^* = p_2|_{v_1=1,\, v_2=0}, \qquad D^* = p_2|_{v_1=0,\, v_2=-1}. \tag{17c, d}$$

Two BEM runs are still needed to get the above four parameters. The first BEM run produces A^* and C^*, while the second BEM run produces B^* and D^*. Nevertheless, only one BEM matrix needs to be solved at each frequency, because the two BEM runs share the same coefficient matrix. The second BEM run uses only a different velocity condition, and therefore, requires only a trivial back-substitution procedure. Actually, the two BEM runs can be done simultaneously because the two right side vectors corresponding to the two different velocity boundary conditions may be formed at the same time. Compared to the three-point method, this improved method is even faster because it does not require any field-point solution

The original four-pole parameters in equations (10) can be obtained by solving equation (16) for p_1 and v_1 in terms of p_2 and v_2. Doing so yields

$$A = A^*/C^*, \qquad B = B^* - A^*D^*/C^*, \tag{18a, b}$$

$$C = 1/C^*, \qquad D = -D^*/C^*. \tag{18c, d}$$

Note that the above equations are identical to the pressure response functions in the papers by Kim and Soedel [9–11]. With the four-pole parameters available, the TL can then be calculated by equation (12). The major advantage of the improved method is that it not only provides a very fast method for computing the TL, but it also produces the four-pole parameters.

6. NUMERICAL RESULTS

Two muffler models are presented in this section to demonstrate the BEM analysis. The first example is a concentric tube resonator with a flow plug in the middle of the perforated tube. The geometry of the muffler is axisymmetric. The details of the model are shown in Figure 3. The internal tube contains both perforated and thin surfaces. The porosity of the first region (L_2) is 21·68%, and the porosity of the second region (L_5) is 13·54%. The internal portions where there is no perforation are all modelled by thin elements (S_t). All the three different empirical formulas for perforated tubes under the no-flow condition (equations (5–7)) are tested in the BEM. The three BEM predictions are compared to experimental data. Figure 4 show the BEM prediction (dashed line) using the Sullivan and Crocker's formula (equation (5)). Also shown in the figure is the experimental TL curve (solid line). From the figure, one can see that the BEM

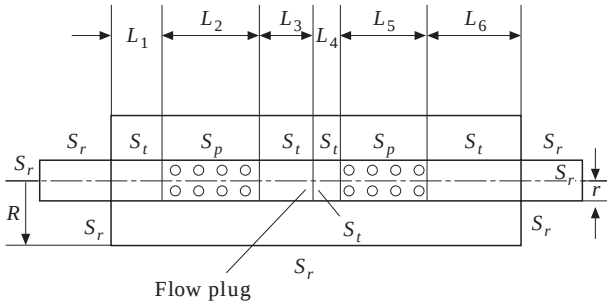

Figure 3. Concentric-tube muffler with a flow plug ($L_1 = 0{\cdot}0317$ m, $L_2 = 0{\cdot}0952$ m, $L_3 = 0{\cdot}0255$ m, $L_4 = 0{\cdot}0063$ m, $L_5 = 0{\cdot}0952$ m, $L_6 = 0{\cdot}0953$ m, $R = 0{\cdot}0538$ m, $r = 0{\cdot}0254$ m). For perforations in L_2: $\sigma = 0{\cdot}2168$, $d_h = 0{\cdot}00635$ m, $t = 0{\cdot}0011938$ m; for perforations in L_5: $\sigma = 0{\cdot}1354$, $d_h = 0{\cdot}00635$ m, $t = 0{\cdot}0011938$ m.

prediction is fairly good except some minor shifts of the peaks. To see if incorporating the effects of hole diameter and wall thickness can improve the accuracy, the same model is run again twice with equations (6) and (7), respectively. Figure 5 shows the two BEM predictions along with the experimental TL curve (solid line). The dotted line in Figure 5 is obtained by using Sullivan's formula (equation (6)), and the dashed line is obtained by using Bento Coelho's formula (equation (7)). It is seen that either equation (6) or equation (7) gives better prediction than equation (5) for this particular muffler model.

The same model is then run with a mean flow with Mach number $M = 0{\cdot}1034$. Since the flow type is cross flow due to the flow plug inserted in the middle of the internal tube, the cross-flow formula by Sullivan (equation (8)) is used in the BEM. However, the convective-flow effect on acoustic wave propagation is totally neglected in the BEM formulation due to the low Mach number. In other words, the governing differentiation equation is still the Helmholtz equation, and the mean flow only comes into effect in the transfer impedance formula for perforated tubes.

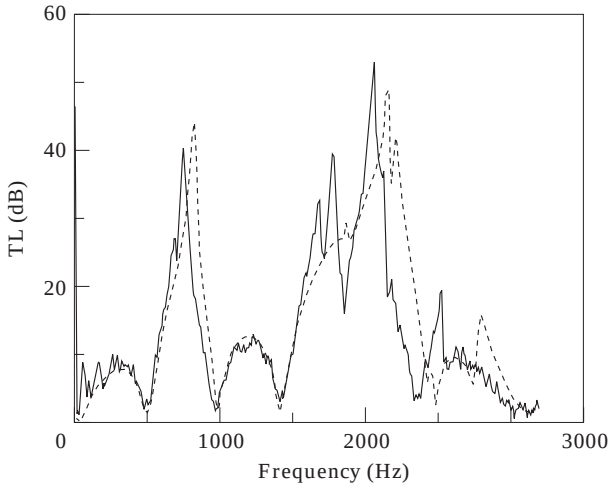

Figure 4. Comparison between the experimental data (——) and the BEM prediction using Sullivan and Crocker's formula (equation (5), - - - - -) for the concentric-tube muffler with a flow plug.

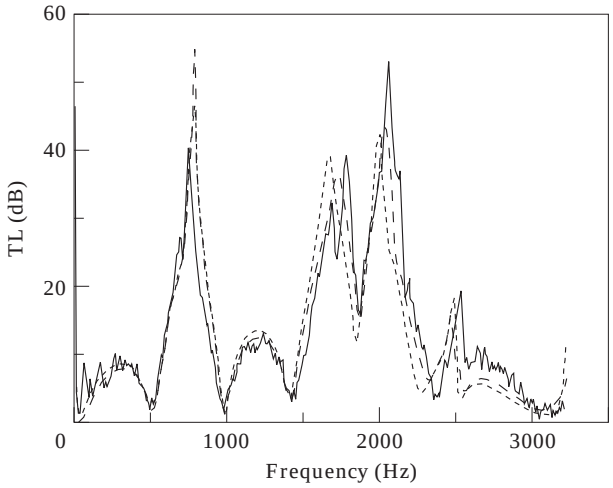

Figure 5. Comparison between the experimental data (——) and the BEM predictions using Sullivan's formula (equation (6), -----) and Bento Coelho's formula (equation (7), – – –) for the concentric-tube muffler with a flow plug.

Figure 6 shows the comparison between the BEM prediction (dashed line) and the experimental TL curve (solid line). It is seen from the figure that equation (8) can yield a decent result even when the convective-flow effect is neglected in the acoustic wave equation.

The second muffler model is a muffler that has two parallel perforated tubes. The details of the model are shown in Figure 7. This model is more complex than the previous one because the geometry is not axisymmetric. Figure 8 shows the BEM prediction (dashed line) using Sullivan and Crocker's formula (equation (5)) along with the experimental TL curve (solid line). To see the effects of hole

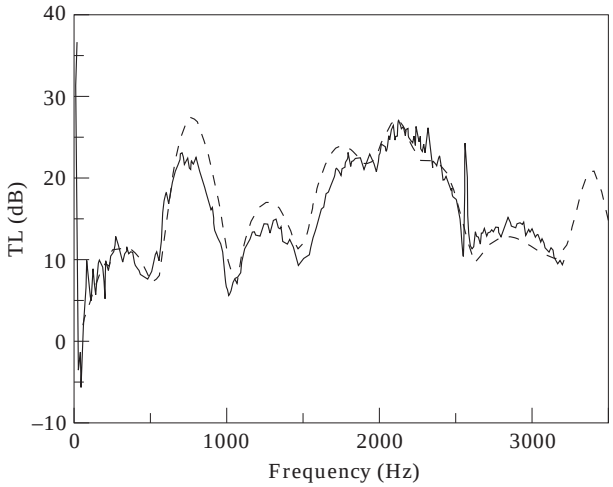

Figure 6. Comparison between the experimental data (——) and the BEM prediction using Sullivan's cross-flow impedance formula (equation (8), – – –) for the concentric-tube muffler with a flow plug when $M = 0{\cdot}1034$.

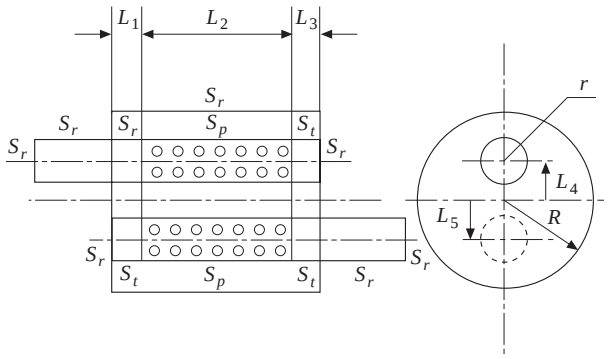

Figure 7. Muffler with two parallel perforated tubes ($L_1 = 0{\cdot}0254$ m, $L_2 = 0{\cdot}4572$ m, $L_3 = 0{\cdot}0254$ m, $L_4 = 0{\cdot}0381$ m, $L_5 = 0{\cdot}0381$ m, $R = 0{\cdot}1016$ m, $r = 0{\cdot}0254$ m). For both tubes: $\sigma = 0{\cdot}144$, $d_h = 0{\cdot}003175$ m, $t = 0{\cdot}0011938$ m.

diameter and wall thickness, the results of using Sullivan's formula (equation (6), dotted line) and Bento Coelho's formula (equation (7), dashed line) are shown in Figure 9. From Figures 8 and 9, one can see that all BEM predictions show fairly good comparison with the experimental curve, although either equation (6) or (7) seems to give a better result than equation (5).

To demonstrate the efficiency of the improved method for deriving the four-pole parameters, the CPU time comparison of the three different TL methods at three individual frequencies is shown. The second muffler model is used as the test case. Since the muffler has a plane of symmetry, one only models one half of the geometry. At 20 Hz, 1000 Hz and 2000 Hz, the number of elements (or nodes) is 322, 469 and 961, respectively. The CPU time comparison on a Pentium 120 notebook computer is shown in Table 1. From the Table, one can see that the improved four-pole method is even a little faster than the three-point method for the 961-node model. Since the entire integral equation is not reformulated for the

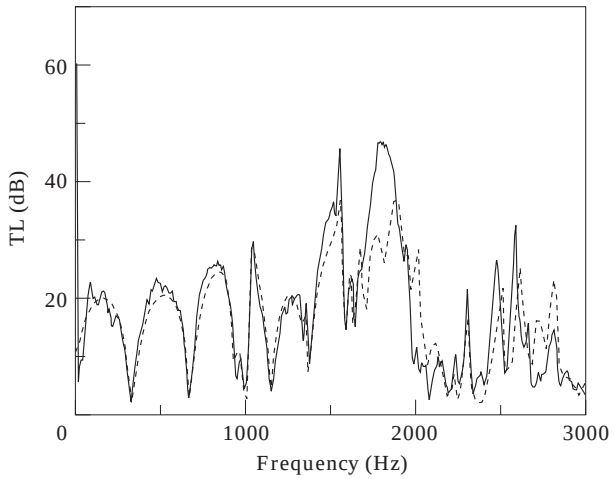

Figure 8. Comparison between the experimental data (——) and the BEM prediction using Sullivan and Crocker's formula (equation (5), -----) for the muffler with two parallel perforated tubes.

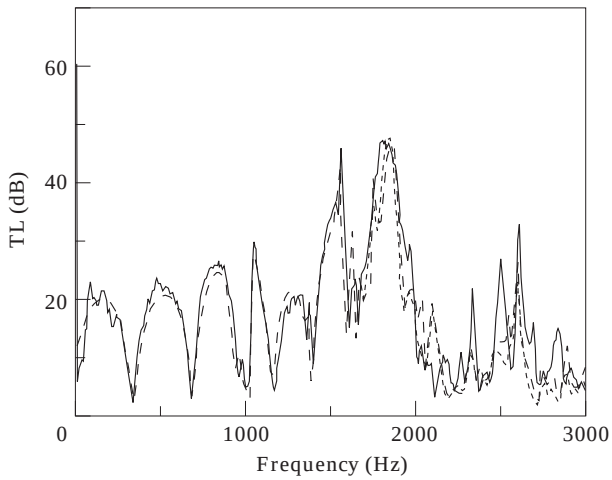

Figure 9. Comparison between the experimental data (——) and the BEM prediction using Sullivan's formula (equation (6), -----) and Bento Coelho's formula (equation (7), – – –) for the muffler with two parallel perforated tubes.

TABLE 1

CPU time (s) comparison of the three different TL methods on a Pentium 120 PC

Number of nodes	Four-pole method	Three-point method	Improved four-pole method
322	85	63	63
469	201	145	146
961	1105	691	687

second BEM run even in the conventional four-pole method the CPU time of the conventional four-pole method is not exactly twice of the three-point method or the improved four-pole method. However, when the frequency goes up and the size of the matrix becomes bigger and bigger, solving the matrix will dominate the entire process. Then, the CPU time of either the three-point method or the improved four-pole method will eventually reach 50% of the conventional four-pole method.

7. CONCLUSIONS

An improved method for deriving the four-pole parameters is presented in this paper to accelerate the TL prediction procedure using the BEM. This improved method uses only the velocity boundary condition at the inlet and the outlet. Although two BEM runs are still needed at each frequency, only one BEM matrix needs to be solved. As a consequence, the improved method is as fast as the three-point method. More importantly, it also produces the four-pole parameters.

Several different transfer impedance formulas for perforated tubes are tested in this paper. Test cases show that all formulas produce fairly good results when compared to the experimental TL curve, although formulas incorporating the effects of hole diameter and wall thickness (equations (6) and (7)) seem to yield better accuracy than the original formula by Sullivan and Crocker (equation (5)).

One test case in this paper also includes a mean flow with $M = 0{\cdot}1034$. The cross-flow impedance formula by Sullivan (equation (8)) is adopted in the BEM to take the mean flow effect into account. However, the convective-flow effect is not included in the acoustic wave equation. Even so, the BEM prediction shows very good comparison with the experimental data.

ACKNOWLEDGMENT

This research was supported by Nelson Industries, Inc.

REFERENCES

1. T. W. Wu and G. C. Wan 1996 *ASME Transaction*, *Journal of Vibration and Acoustics* **118**, 479–484. Muffler performance studies using a direct mixed-body boundary element method and a three-point method for evaluating transmission loss.
2. C. Y. R. Cheng, A. F. Seybert and T. W. Wu 1991 *Journal of Sound and Vibration* **151**, 119–129. A multidomain boundary element solution for silencer and muffler performance prediction.
3. Z. H. Jia, A. R. Mohanty and A. F. Seybert 1882 *Proceedings of the Second International Congress on Recent Developments in Air- and Structure-Borne Sound and Vibration*, M. J. Crocker and P. K. Raju (eds.), 957–964. Numerical modeling of reactive perforated mufflers.
4. C. N. Wang, C. C. Tse and Y. N. Chen 1993 *Engineering Analysis with Boundary Elements* **12**, 21–27. A boundary element analysis of a concentric-tube resonator.
5. Z. Ji, Q. Ma and Z. Zhang 1994 *Journal of Sound and Vibration* **173**, 57–71. Application of the boundary element method to predicting acoustic performance of expansion chamber mufflers with mean flow.
6. J. Igarashi and M. Toyama, 1959 *Aeronautical Research Institute*, *University of Tokyo*, *Report No*. 339. Fundamentals of Acoustical Silencers (I)—Theory and Experiments of Acoustic Low-Pass Filters.
7. M. L. Munjal 1987 *Acoustics of Ducts and Mufflers*. New York: Wiley-Interscience.
8. G. C. Wan 1995 *Proceedings of the* 1995 *International Conference on Noise Control Engineering*, 421–424. Prediction and measurement of the acoustic performance of mufflers.
9. J. Kim and W. Soedel 1989 *Journal of Sound and Vibration* **129**, 237–254. General formulation of four pole parameters for three dimensional cavities utilizing modal expansion with special attention to the annular cylinder.
10. J. Kim and W. Soedel 1989 *Journal of Sound and Vibration* **131**, 103–114. Analysis of gas pulsations in multiply connected three dimensional acoustic cavity with special attention to natural mode or wave cancellation effects.
11. J. Kim and W. Soedel 1990 *ASME Transactions*, *Journal of Vibration and Acoustics* **112**, 452–459. Development of general procedure to formulate four pole parameters by modal expansion and its application to three dimensional cavities.

12. J. W. Sullivan and M. J. Crocker 1978 *Journal of the Acoustical Society of America* **64**, 207–215. Analysis of concentric-tube resonators having unpartitioned cavities.
13. J. L. Bento Coelho 1984 *Proceedings of* 1984 *Nelson Acoustics Conference*, Modeling of cavity backed perforate liners in flow ducts.
14. J. Hadamard 1923 *Lectures on Cauchy's Problem in Linear Partial Differential Equations*. New Haven: Yale University Press.
15. G. Krishnasamy, L. H. Schmerr, T. J. Rudolphi and F. J. Rizzo 1990 *ASME Transactions*, *Journal of Applied Mechanics* **57**, 404–414. Hypersingular boundary integral equations: some applications in acoustic and elastic wave scattering.
16. K. N. Rao and M. L. Munjal 1986 *Journal of Sound and Vibration* **108**, 283–295. Experimental evaluation of impedance of perforates with grazing flow.